eXPRESS Polymer Letters Vol.12, No.7 (2018) 628–639
Available online at www.expresspolymlett.com
https://doi.org/10.3144/expresspolymlett.2018.53

Improving the performance of UV-curable coatings with carbon nanomaterials

Y. Jiang[1], *S. Y. Zhang*[2,3], *X. L. Zhang*[3], *T. Zhang*[1*]

[1]College of Engineering and Applied Sciences, Nanjing University, 210093 Nanjing, China
[2]Department of Macromolecular Science, Fudan University, 200433 Shanghai, China
[3]Guangzhou Wraio Chemical Material Co., Ltd., 510726 Guangzhou, China

Received 27 December 2017; accepted in revised form 16 February 2018

Abstract. By combining a trifunctional urethane acrylate synthesized from a hexamethylene diisocyanate trimer and caprolactone acrylate with a bifunctional urethane acrylate prepared from hydroxyethyl acrylate and isophorone diisocyanate, a new reactive resin mixture was prepared, and trimethylolpropane triacrylate was chosen as the thinner to constitute a novel coating matrix. Different amounts of multi-functionalized carbon nanotubes (CNTs) and graphene oxide (GO) were introduced into the matrix and cured by ultraviolet radiation, producing different coatings. Utilizing the methods of Fourier transform infrared (FTIR) spectroscopy, ultraviolet-visible (UV-VIS) spectroscopy, wide angle X-ray diffraction (WAXS) and thermogravimetric analysis (TGA), the chemical structures and physical properties of the coatings were analyzed. A series of ASTM methods, such as pencil hardness classification, RCA abrasion, crosscut adhesion test classification, and chemical resistance rub testing, were applied to investigate the performances of the coatings. It was found that introducing a small amount of carbon nanomaterials can improve the thermal stability, surface hardness, adhesion, abrasive resistance, and chemical resistance performance of the UV-curable coatings. The reasons and mechanisms of the performance improvements are discussed in this work.

Keywords: *nanomaterials, polyurethane acrylate, UV-curable coating, carbon nanotube, graphene oxide*

1. Introduction

Along with the continually increasing concerns on environmental protection, energy consumption and occupational health and safety, radiation curing technologies, including ultraviolet (UV) and electron beam curing, have received increasing attention in the last several decades. After its invention in the 1960s [1], the UV curing technology is much better known for its 5E characteristics (efficient, enabling, economical, energy saving and environment friendly) and has been widely applied in various industries, including paints, printing, packaging, surface protection and finishing, and device manufacturing in the form of products such as ink, coatings and adhesives [2, 3]. Even in the rising 3D-printing market, the applications of UV-curing technology have exhibited a rapidly growing trend [4]. Currently, UV-curable coatings have the biggest share in the entire UV curing product market [3].

A typical UV-curable formulation consists of reactive resins (oligomers or prepolymers) and reactive thinners, which are also called monomers. Due to the chemical reaction, the thinner is tightly linked to the polymer matrix, thus contributing to the formation of the crosslinked coating film. The power density of the UV radiation by itself is not sufficient to achieve polymerization. For that reason, photo initiators or photo sensitizers are mixed into the coating to initiate the polymerization process, which is also known as curing the coating [3]. The performances of the resulting

*Corresponding author, e-mail: ztnj@nju.edu.cn

coatings, such as the surface hardness, adhesion to substrate, chemical resistance property, gloss and abrasive resistance, are determined by the particular formulation of the coating system. The most common reactive resins include the various multi-functional acrylates, e.g., the polyurethane acrylates, epoxy acrylates, polyester or polyether acrylates, and vinyl resins [3]. The chemical structures and physical properties of these resins are reflected as the degree of functionality, molecular weight, flexibility, crystallinity and even the stability, as determined by the structures and performances of the cured coating. For reactive thinners, dozens of monomers with single, double and triple reactive groups (e.g., double bonds) in a molecule are commercially available. The permutation and combination of the resins and the monomers, supplemented with various additives, photo initiators and different process conditions have led to millions of possible formulations to meet all types of requirements in various fields. In 2015, 467.9 kilo-tons of reactive resins were produced worldwide, with a value of 2.21 billion US dollars. By 2024, the output will reach 1000 kilo-tons, with a value of 4.67 billion US dollars.

However, the requirements for the ingenuous formulation designs and performance improvements in UV-curable coatings are growing continuously, along with the expansion of their potential applications. In this paper, carbon nanotubes (CNTs) and graphene oxide (GO) were incorporated into polyurethane acrylate to formulate a UV-curable coating formulation with a facile synthesis and preparation and improved performance. It is well known that CNTs and GO are typical carbon nanomaterials with a 1D fibrous structure and 2D plate structure, respectively. The introduction of CNTs into a UV-curable polymer matrix was first reported in microelectromechanical system applications [5] and then expanded rapidly into UV-curable coating research [6–13]. At the same time, various chemical modifications have been applied to GO [14–23] to ensure the homogeneous dispersion in organic coating systems and endow the produced coating with specific properties. In general, it is desirable to provide performance improvements by introducing nanomaterials into various polymers [24] or the organic coating. Examples of improved properties include the surface hardness, adhesion, abrasive resistance, chemical resistance, etc.

In this paper, a trifunctional urethane acrylate composed of a hexamethylene diisocyanate trimer ($(HDI)_3$) and caprolactone acrylate (HECLA) mixed with a bifunctional urethane acrylate synthesized from hydroxyethyl acrylate (HEA) and isophorone diisocyanate (IPDI) was used as the reactive resin. Trimethylolpropane triacrylate (TMPTA) was chosen as a thinner to constitute a novel matrix of UV-curable coatings. The carbon nanomaterials, CNTs and GO, were functionalized by an acrylate reaction with IPDI and HEA and were introduced into the matrix at various quantities.

It was expected that the unsymmetrical 1D fibrous structure of CNTs and 2D plate structure of GO may introduce special performance. Also the huge specific surface area of carbon nanomaterial are also expectable to enhance the interactions between the nano-fillers and polymer matrix thus improve the performances of the final compositions. The chemical structures, physical properties and performances of the obtained coating were characterized, analyzed and investigated. In particular, the coating performance was a focus, and the effects of the type and amount of carbon nanomaterials are discussed.

2. Experiments

2.1. Materials

Hexamethylene diisocyanate trimer ($(HDI)_3$) is an industrial product (trade name Wannate HT-100 with NCO content of 21.7–22.2%) of the Wanhua Chemical Group Co., Ltd. (Yantai, China). Caprolactone acrylate (HECLA) was provided by KPX Green Chemical Co., Ltd. (Seoul, Korea), with a trade name of Komerate-C021. Isophorone diisocyanate (IPDI) was purchased from China Branch of Evonik Industries AG (Shanghai, China), with a trade name of Vestanat IPDI and a purity ≥99.5%. Hydroxyethyl acrylate (HEA) was provided by Anhui Renxin Environmental Protection Materials Co., Ltd. (Xuancheng, China) as an industrial product (purity ≥97%). Graphene (KNG-G5) was purchased from Xiamen Knano Graphene Technology Co. Ltd. (Xiamen, China), with a diameter ranging from 5 to 20 μm and a thickness of 1–5 graphene layers. Multi-walled CNTs with diameters of 10–30 nm and lengths of 5–15 μm were purchased from Shenzhen Nano-Technologies Port Co., Ltd. (Shenzhen, China) and were prepared via chemical vapor deposition (CVD) with a La–Ni catalyst and a purity no less than 95% with 3–5% amorphous carbon. The chemicals, such as dibutyltin dilaurate (DBTL), 2,6-Di-tert-butyl-4-methylphenol (BHT) and trimethylolpropane triacrylate (TMPTA),

were kindly provided by Guangzhou Wraio Chemicals (Guangzhou, China) as industrial products. The photoinitiator Irgacure 184 ((1-hydroxycyclohexyl) phenyl-methanone) and Irgacure TPO (diphenyl-2,4,6-trimethylbenzoyl-phosphine oxide) are products of Ciba-Geigy (a subsidiary corporation of the BASF) and were provided by Guangzhou Wraio Chemicals. The silicone-containing surface additive BYK-333 is a product of BYK Additives & Instruments (German) and provided by Guangzhou Wraio Chemicals. The other chemicals, such as KMnO4, $NaNO_3$, H_2SO_4 (Purity ≥ 98%), H_2O_2 (30%), and Hydrochloric acid (HCl, 38%) were purchased from Nanjing Reagent Co. Ltd. (Nanjing, China) and used as received. *N*,*N*-dimethylformamide (DMF, purity ≥ 99.5%) was purchased from Nanjing Reagent Co. Ltd. (Nanjing, China), dried with a molecular sieve and distilled under a reduced pressure.

2.2. Synthesis and preparation

The tri-functional polyurethane acrylate $(HDI\text{-}HECLA)_3$ was synthesized as Figure 1 and used as the main matrix of the UV-curable coating. In detail, 167 g of (0.33 mol) $(HDI)_3$ was allowed to react with 333 g of (1 mol) HECLA with 0.05% of DBTL as the catalyst and 0.2% BHT as the inhibitor. The residual isocyanate groups (NCO value) in the products were determined as having a value lower than 0.2%. The graphene powder (KNG-G5) and carbon nanotubes were first oxidized following the modified method of Hummers [25] using $KMnO_4$, H_2SO_4, and H_2O_2, which brought the carboxy and hydroxy groups onto the carbon nanomaterials and made it reactive with the isocyanate groups.

To homogenously disperse the nanomaterials into the UV-curable coating system, modified GO and CNTs were reacted with the acrylate system according to Figure 2. First, 22.2 g of (0.1 mol) IPDI mixed with 0.01 g DBTL and 0.04 g of BHT were added to a four-neck flask equipped with a magnetic stirring and a thermometer. With continuous stirring, 11.6 g of (0.1 mol) HEA was added dropwise, and the temperature of the reaction system was consistently kept lower than 50 °C by controlling the feeding rate of the HEA. This process took approximately 1 hour to add the HEA, after which the reactions were stirred continually to allow the reaction to continue for 1 more hour at 45–50 °C. The reaction resulted in the monofunctional urethane acrylate resin (IPDI-HEA) for future reactions. Then, 2 g of GO pre-dispersed in 52.6 g of dried DMF by ultrasonication was added to the mixture and continual stirring for 12 hours at 45–50 °C. Finally, an additional 11.6 g (0.1 mol) HEA were added and reacted for 3 more hours at the same temperature, resulting in a GO-HEA_x dispersion with a concentration of 2% by weight in HEA-IPDI-HEA/DMF solution. In an analogous manner, CNT-HEA_y dispersed in DMF using the same concentration were also synthesized. The same synthesis procedure was carried out, but no carbon nanomaterials were added, which resulted in the bifunctional urethane acrylate HEA-IPDI-HEA.

Based on Table 1, various amounts of trifunctional $(HDI\text{-}HECLA)_3$ acrylate resin, HEA-IPDI-HEA bifunctional acrylate resin, 2% GO-HEA_x in DMF or 2% CNT-HEA_y in DMF, photoinitiator Irgacure 184 and Irgacure TPO, reactive diluents TMPTA and leveling agent BYK-333 were mixed with a high-speed

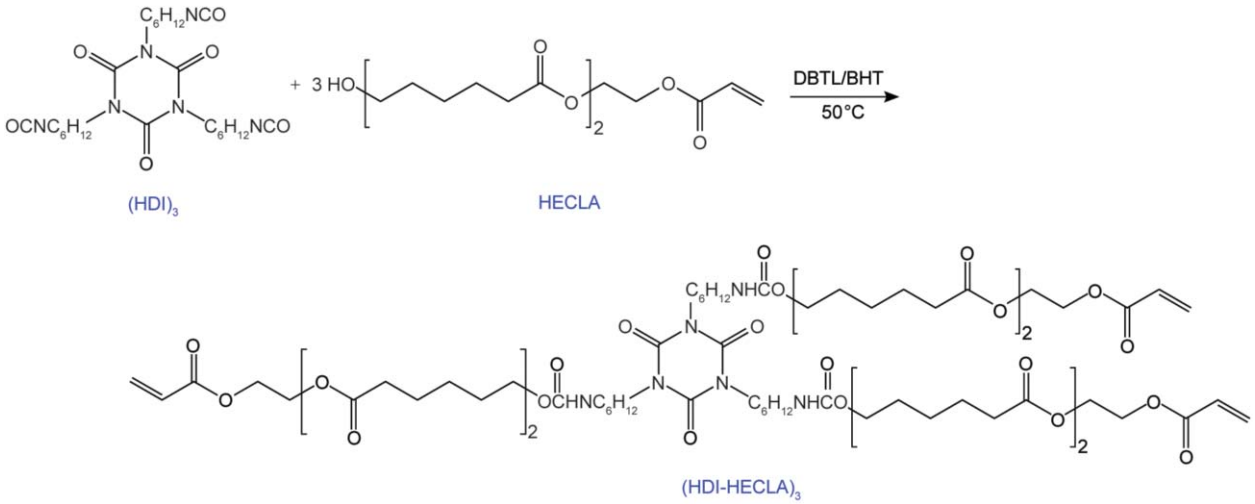

Figure 1. Synthesis of trifunctional polyurethane acrylate.

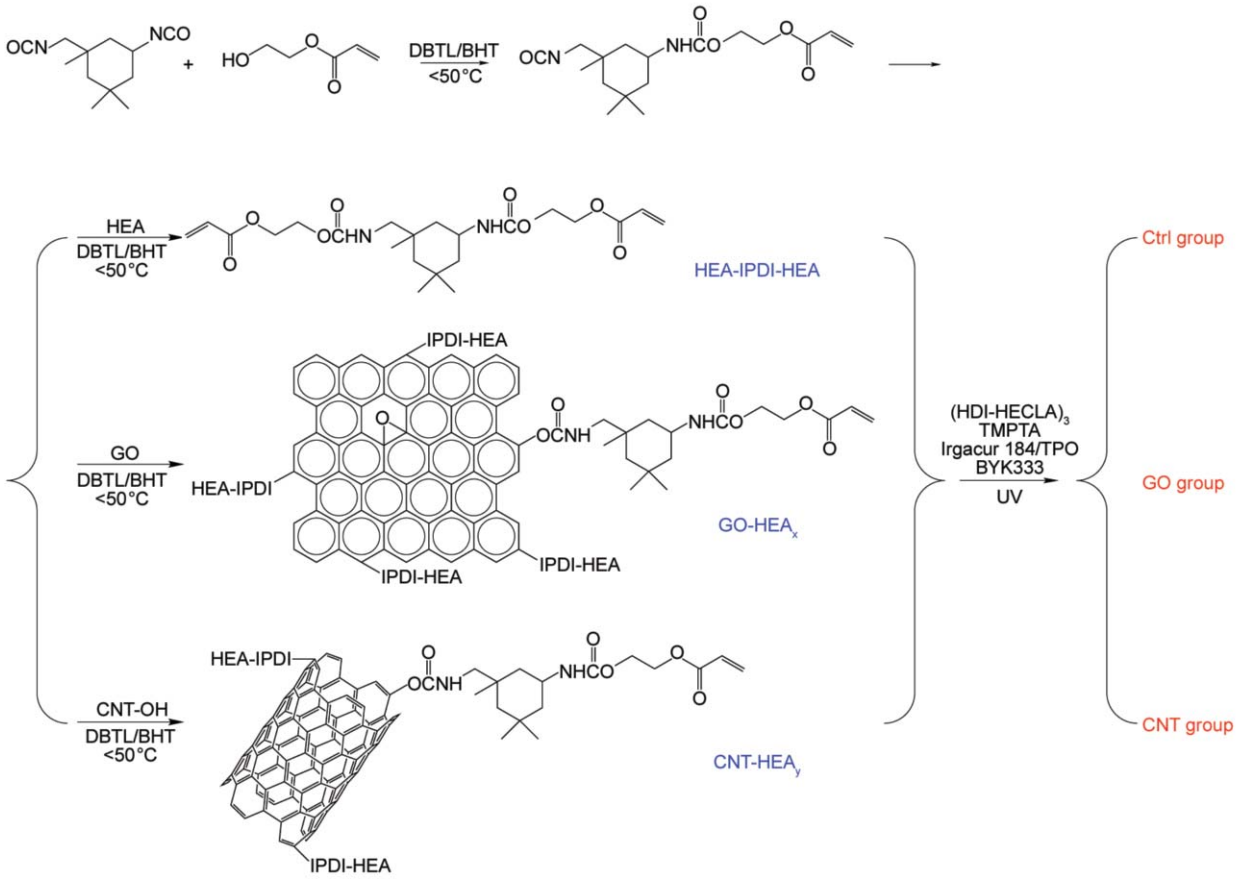

Figure 2. Synthesis and preparation route of modified carbon nanomaterials and coating samples.

Table 1. Mixture formulations for spray coatings.

Sample code[a]	Actual concentration of GO or CNTs in the coating samples [calculated % in mass]	$(HDI\text{-}HECLA)_3$ [g]	HEA-IPDI-HEA [g]	2% GO-HEA_x in DMF [g]	2% CNT-HEA_y in DMF [g]
0.2Ctrl	/	90	10	/	/
0.4Ctrl	/	80	20	/	/
0.6Ctrl	/	70	30	/	/
0.8Ctrl	/	60	40	/	/
1.0Ctrl	/	50	50	/	/
0.2GO	0.168	90	/	10	/
0.4GO	0.351	80	/	20	/
0.6GO	0.552	70	/	30	/
0.8GO	0.774	60	/	40	/
1.0GO	1.019	50	/	50	/
0.2CNT	0.168	90	/	/	10
0.4CNT	0.351	80	/	/	20
0.6CNT	0.552	70	/	/	30
0.8CNT	0.774	60	/	/	40
1.0CNT	1.019	50	/	/	50

[a]in every sample, 20 g of TMPTA, 2 g of Irgacure 184, 2 g of Irgacure TPO and 0.4 g of BYK-333 were also included.

mixer, followed by adding a suitable amount of DMF to regulate the viscosity of the mixtures. The mixtures were then sprayed onto polycarbonate (PC) sheets, dried at 60 °C for 5 minutes, and cured under a UV lamp with an exposure energy of 800 mJ/cm^2. The final coatings on the PC sheets were approximately 20 μm thick and stored at room temperature for further studies.

2.3. Characterization and performance testing

The Fourier transform infrared (FTIR) spectra were recorded on a PE GX spectrometer (Perkin-Elmer, USA) at room temperature on KBr pellets with sample concentrations of ~1% from 4000 to 400 cm^{-1} at a resolution of 4 cm^{-1}. In order to investigate the microstructure of nanomaterials in the coating matrix, the coating membranes containing 1.0% CNT and GO were peered off from the PC substrates and fractured in liquid nitrogen. All the section of samples with gold coating (approx. 40 nm thickness) were observed by SEM (S-3400 N II, HITACHI, Japan) at an acceleration voltage of 20 kV. The UV-vis spectra of the coating films were evaluated by MAPADA UV-1800PC (Shanghai, China) with wavelengths ranging from 200–600 nm. Wide angle X-ray diffraction (WAXD) measurements were performed on a Rigaku ULTIMA-3 setup, with a Mar 345 image plate used as the detector, Cu Kα as the source (wavelength of 0.1542 nm), a recorded region of 2θ from 5 to 40°, and a scanning speed of 2°·min^{-1}. Thermogravimetric analysis (TGA) results were recorded on a Netzsch STA409PC (Selb, Germany) in a N_2 atmosphere at a heating rate of 20 °C/min from room temperature to 600 °C. The pencil hardness of the UV-cured coating was determined using ASTM D3363-05. The crosscut adhesion tests were performed according to ASTM D3359-08 and the Test Method B were performed. In detail, a BGD504/2 crosscut adhesion test blade (Biuged Laboratory Instruments, Guangzhou, China) were used to cut the cross grid with 1.0 mm spacing and then 3M Scotch transparent film tape 600 were covered for 90 s and then removed. The results were classified as 0-5B according to the percentage of area removed. The RCA abrasion tests were carried out following ASTM F2357-10 with a BGD530 RCA abrasion wear tester (Biuged Laboratory Instruments, Guangzhou, China) with force of 175 g. The gloss measurements were performed at 60.2° with a BGD512 Glossmeter (Biuged Laboratory Instruments, Guangzhou, China) according to ASTM D523-14. The solvent (ethanol and butanone) resistance of the coatings was investigated using solvent rubs (ASTM D5402-15) with a BGD525 alcohol abrasion tester (Biuged Laboratory Instruments, Guangzhou, China). The boiling resistance tests were carried by boiling multiple samples in water at 100 °C, one of the samples was taken out and check by crosscut adhesion tests every 30 min, The results were recorded as the crosscut adhesion class after been boiled for few hours.

3. Results and discussion

3.1. Chemical structure analysis by FTIR

Figure 3a showed the FTIR spectra of raw, intermediate and final trifunctional polyurethane acrylate of $(HDI\text{-}HECLA)_3$. For the spectrum of $(HDI)_3$, the absorption peak at 2260 cm^{-1} represented the specific stretching vibration peak of N=C=O group, which was also shown in the mixture of $(HDI)_3$ and HECLA before the reaction. While the peak at 1680 cm^{-1} was the absorption peak of C=O group which was kept in the mixture and the final PUA resin. For HECLA, the most obvious peak at 1725 cm^{-1} represented the typical absorption of acrylate group, which was always kept in the mixture and the final trifunctional PUA resin. Comparing the spectra of the mixture and the final PUA resin, the disappearance of the peak at 2260 cm^{-1} indicated the complete reaction of NCO group in $(HDI)_3$ and OH group in HECLA and the successfully synthesis of final trifunctional PUA resin. To confirm the chemical modifications from the carbon nanomaterials, the crude GO and CNTs products that reacted with IPDI and HEA were thoroughly

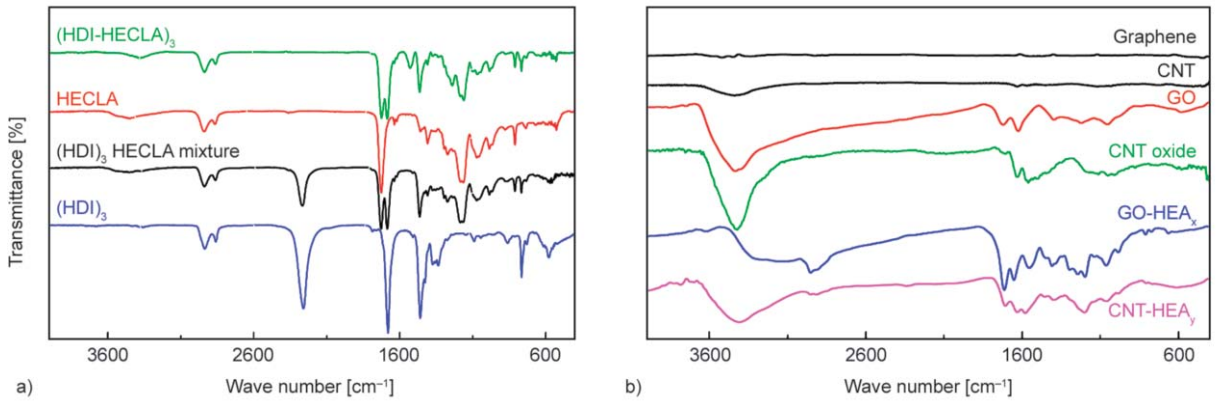

Figure 3. FTIR spectra of raw, intermediate and final products of $(HDI\text{-}HECLA)_3$ (a) and modified carbon nanomaterials (b).

washed with ethanol. The obtained solid products, GO-HEA$_x$ and CNT-HEAy were vacuum dried at room temperature and scanned with FTIR along with the raw carbon nanomaterials and intermediate products, as shown in Figure 3b. For the graphene and raw CNTs, the curves are almost straight lines, except for a slight absorption that appears at approximately 3500 cm^{-1} for the defects of the multiple-walled structure. The oxidation of the GO and CNT oxide in sulfuric acid provides a typical carboxylic group absorption peak at 1600–1700 cm^{-1} and absorbance at approximately 1050 cm^{-1}, which corresponds to the other side groups that contain C–O bonds, such as epoxy and hydroxyl. The relatively large absorption peak at approximately 3500 cm^{-1} is obviously from the hydroxyl groups. Further reactions with IPDI and HEA reduced the absorbances of the hydroxyl groups at high wavenumbers but generated a series of absorption peaks from 700–1100 cm^{-1}, which are associated with the typical organic structures, such as carbonyl, ester, and ether, and correspond to bonds such as C–O, C–H, C=O, and C–O–C. The obvious spectrum changes of the FTIR from the raw carbon nanomaterials in the final products proved the successful modification on the pristine graphene and nanotubes.

3.2. Appearance, microstructure and physical properties investigation

After HEA-IPDI-HEA or modified carbon nanomaterials have been incorporated with (HDI-HECLA)$_3$, TMPTA, BYK333 and the photo initiators, the coating system exhibited a homogenous state. After dilution by DMF, the coating solution was sprayed on the polycarbonate substrate, dried for 5 minutes, and cured under a UV lamp with an exposure energy of 800 mJ/cm^2.

Figure 4a presents the images of the UV-cured coatings. The control coating films without carbon materials were transparent, but the samples with carbon nanomaterials showed an increasing chromaticity with increasing amounts of CNTs and GO. For the CNT samples, the coating showed an increasing grayscale, and the color become darker. For GO, the coatings became brown, and the color also grew deeper. Figure 4b and 4c shows the SEM micrographs of the section of the coating incorporated with 1.0% in mass of CNT and GO respectively. We tried to observe the distribution of carbon nanomaterials in UV-cured matrix by transmission electron microscopy (TEM), but the coating was too thick to be penetrated by electrons. Thus, the coating membranes were fractured in liquid nitrogen and the

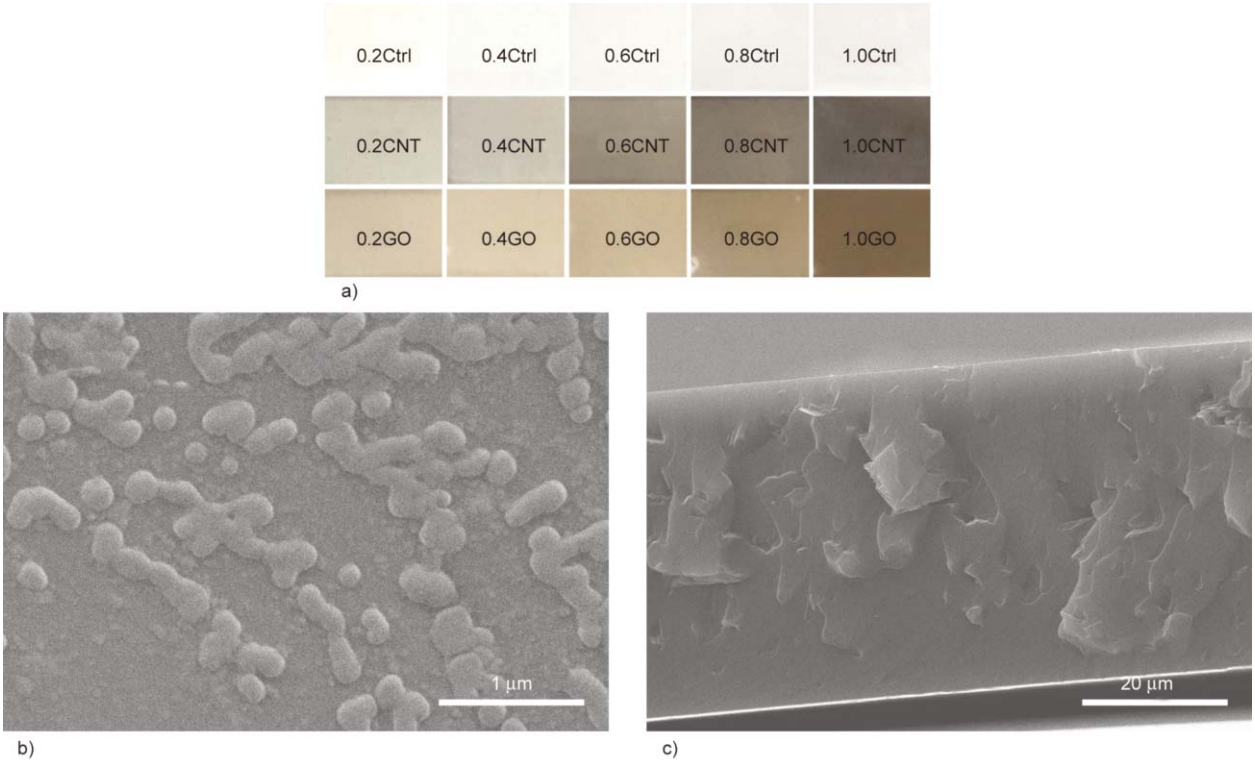

Figure 4. Images of UV-cured coatings with and without carbon nanomaterials (a), the SEM of section of coating containing 1.0 wt% CNT (b) and GO (c). The bar in (b) and (c) are 1 µm and 20 µm respectively.

cross-sections were observed by SEM. In Figure 4b, the fibrous structures with the diameter of about 100 nm correspondence to the modified CNT were observed and the typical images presented the homogeneous distribution of CNT in the coating matrix. While in Figure 4c, the lamellar structures caused by modified GO sheets were also observed clearly.

Figure 5a shows the quantitative UV-Visible spectra of the coating film with 1.0% carbon nanomaterials. In the visible range from 400 to 600 nm, the coatings without carbon nanomaterials are nearly colorless and have a transmittance higher than 90%. For the coating films containing 1.0% CNT, the transmittance is approximately 50–60%. For the GO group, the color is deeper than that of both the Ctrl group and CNT group, with a transmittance that decreases to 30–50%. The higher absorbance in the 300–500 nm range leads to a brown appearance of the coating films. The darker chromaticity of the coating containing carbon nanomaterials is not suitable for situations where colorlessness and transparency are important. However, for color coatings, the incorporation of carbon nanomaterials can potentially be applied.

The introduction of CNTs and GO into UV-curable coatings changed the microstructure of the coating matrix. WAXD was used to investigate the crystallization of films, as shown in Figure 5b. From the curves, it was found that even when the incorporated carbon nanomaterials were at a weight percent as high as 1.0%, the WAXD pattern did not present an obvious change. The UV-cured coatings exhibit a semi-crystalline state.

Figure 6 shows the thermogravimetry curves of the UV-coating film samples. As shown in Figure 6, the degradation process and thermal stability were dependent on the chemical structures of the samples. The degradation process of the coating films could be divided into 3 steps. The thermal degradation of the polyurethane acrylate films with bifunctional HEA-IPDI-HEA occurred in the temperature range of 160–280 °C for the first step, at 280–400 °C for the second step, and at 400–450 °C for the third step. The low degradation temperature, especially for the HEA-IPDI-HEA, was mainly attributed to fewer stable urethane groups existing in the aliphatic polyurethane acrylates, which could decompose to form alcohol and isocyanate groups. The results obtained here agree with the literature [26, 27]. Additionally, with the introduction of additional multi-functional modified CNT and GO, more bifunctional HEA-IPDI-HEA was injected, which led to a decrease in the thermal stability. In Figure 6d, the onset main decomposition temperature of the Ctrl group decreased by approximately 20 °C when changing from a 10 to 50% mass ratio of bifunctional HEA-IPDI-HEA. This trend was also investigated in the CNT and GO groups. However, the addition of multi-functional modified CNTs and GO reversed the trend to a certain degree. For every addition, the coating film containing CNTs and GO presented a higher onset decomposition temperature than did the corresponding coating film without CNTs and GO. Comparing the onset decomposition temperatures of the CNT and GO group where they began decomposing, for every addition, no significant differences were found. This result indicates that the introduction of CNTs and GO can improve the thermal stability of the polyurethane acrylate UV-curable coating system.

In general, the thermal degradation of the polyurethane acrylate is associated with changes in the C=O

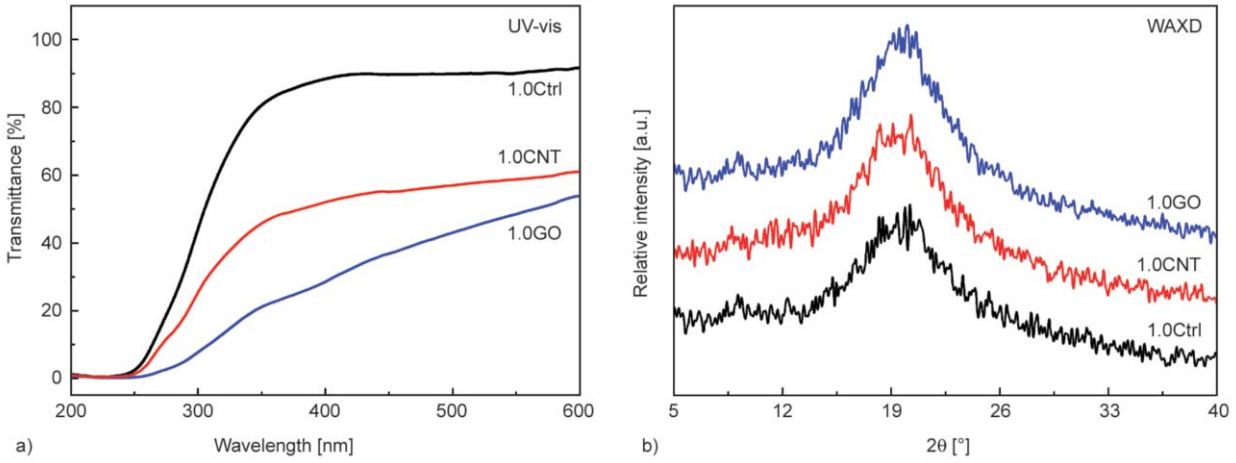

Figure 5. UV-visible spectra (a) and WAXD curves (b) for typical coating films.

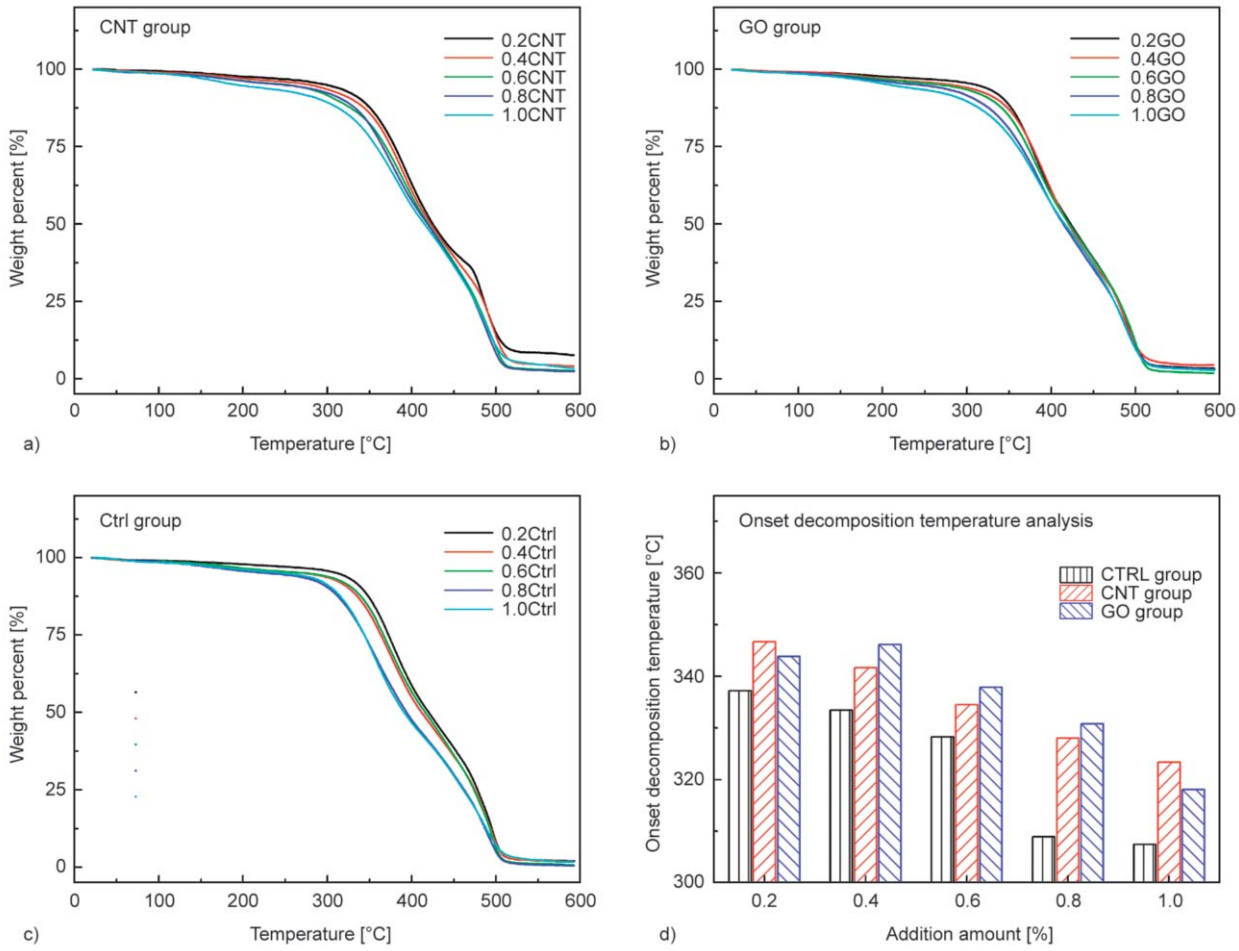

Figure 6. Thermogravimetry analysis of UV-cured coatings of the (a) CNT group, (b) GO group, and (c) Ctrl group; and (d) the onset decomposition temperature analysis results.

and C–N urethane groups. Additionally, some urea compounds may be formed during the thermal degradation of polyurethane acrylate at a high temperature. The enhancement of the thermal stability can be attributed to the higher overall crosslinking density caused by the multi-functional modified CNTs and GO. The crosslinking density of the UV-cured films increased with the increasing functionality of the modified carbon nanomaterials, which may have induced the higher thermal stability in the coating films with multi-functional CNT-HEA_x and GO-HEA_y. Moreover, the thermal stability of the CNT and GO themselves was much higher than that of the polyurethane acrylate, which could also have improved the thermal stability of the coating films, even with a concentration as low as 0.2% in mass.

3.3. Coating performance testing by ASTM methods

As a kind of UV-curable coating, various typical performances were investigated in non-controversial ways according to the ASTM standard, as summarized in Table 2.

The pencil hardness class depends mainly on the chain flexibility of the molecule and crosslinking density of the coating [28]. Specifically, the improved flexible structure of the oligomer leads to a reduction in the hardness of the film, but the improved crosslinking density of the coating film causes the opposite effect. In general, a curing film with good flexibility and a low crosslinking density produces a poor pencil hardness, but the properties of good hardness would be obtained with a poor flexibility and high crosslinking density. In our system, the content of the double bond of the system determines the crosslinking density, and the HECLA moiety dictates the flexible structure of the film. The structure of the CNT and GO group coating films were composed mainly of trifunctional $(HEA\text{-}HECLA)_3$ and bifunctional HEA-IPDI-HEA, with small amounts of multi-functional carbon nanomaterials. In the Ctrl group, with an increase in the amount of bifunctional

Table 2. Performances of UV-cured coatings on polycarbonate sheets.

Sample codes	Pencil hardness class	Crosscut adhesion class	RCA abrasion (counts)[a]	Ethanol resistance rub (counts)[b]	Butanone resistance rub (counts)[b]	Boiling resistance[c]	Gloss [°]
0.2Ctrl	1B	5B	320	4	5	5B/2.5 h; 4B/3 h	91.0
0.4Ctrl	1B	5B	350	6	7	5B/2 h; 3B/2.5 h	91.9
0.6Ctrl	HB	5B	390	7	10	5B/2 h; 2B/2.5 h	91.6
0.8Ctrl	HB	5B	410	8	>10	5B/1.5 h; 4B/2 h	91.2
1.0Ctrl	HB	5B	450	>10	>10	5B/1.5 h; 3B/2 h	92.0
0.2GO	HB	5B	470	2	3	5B/2.5 h; 4B/3 h	89.3
0.4GO	HB	5B	530	1	4	5B/4 h; 3B/4.5 h	88.2
0.6GO	HB	5B	560	3	7	5B/5 h	87.4
0.8GO	F	5B	570	3	7	5B/5 h	81.3
1.0GO	F	5B	460	3	6	5B/4 h; 4B/4.5 h	67.3
0.2CNT	HB	5B	490	1	3	5B/2.5 h; 4B/3 h	89.0
0.4CNT	HB	5B	520	1	4	5B/4 h; 4B/4.5 h	87.6
0.6CNT	HB	5B	550	2	5	5B/5 h	87.2
0.8CNT	F	5B	600	5	9	5B/5 h	84.0
1.0CNT	F	5B	440	2	7	5B/4 h; 2B/4.5 h	61.0

[a]Recorded as the number of rubs when the coating wears out.
[b]None of samples presented the phenomena of whitening and blistering. The number is the count of scratches after the solvent resistance rub testing.
[c]The results recorded as the crosscut adhesion class after been boiled for few hours. For example, 5B/2.5 h represents that the coating's crosscut adhesion class is 5B after boiling for 2.5 h.

HEA-IPDI-HEA, the crosslinking density was decreased, but the flexible HECLA moieties were replaced by short and rigid HEA-IPDI-HEA segments. Thus, the pencil hardness class increased from 1B to HB. By introducing multi-functional modified nanomaterials, the crosslinking density increased further, leading to the further improvement of the hardness. The pencil hardness class was found to begin from HB and ultimately reached F. Between the CNT and GO groups, there was no significant difference in the pencil hardness found, which indicates that the fibroid CNT and sheet GO can both improve the hardness performance of the coating film.

The crosscut adhesion class expressed the adhesive performance of the UV-cured coating. The resulting 5B class represented the highest class of adhesion, which means that no area was removed by the tape and no flaking occurred. These results indicate that all of the samples in our system presented excellent adhesive performance on the PC substrate and that the limited increase (from 1B to F) of the surface hardness did not lead to the complete hardening of the coating film, which often leads to a decrease in the adhesive performance.

The abrasive test is an accurate and repeatable way to determine the abrasion wear characteristics of inks and coatings [27]. The RCA abrasion test presents the combined properties of surface hardness, rigidity and adhesion of the surface coating and is typically used in the 3C (Computer, Communication and Consumer Electronics) industry to the test surface for resistance to abrasion and wear. In general, the RCA abrasion in every group shows improvement with an increasing amount of rigid HEA-IPDI-HEA segments. In the Ctrl group, the highest increase reached 40%. Comparing the samples in different groups, the RCA abrasion was markedly increased when the modified multi-functional carbon nanomaterials were introduced, which can be attributed to the increased crosslinking density and, equally importantly, to the rigidity of the carbon nanomaterials themselves. In addition, the CNTs and GO show no significant difference in improving the RCA abrasion of our system. However, when the carbon nanomaterials were introduced with as much as 1.0% in mass, the RCA abrasion of the CNT and GO groups decreased dramatically, to the same level expressed by the corresponding sample in the Ctrl group. These phenomena are attributed to the phase separation caused by the aggregation of the nanomaterials. When the amounts of nanomaterials exceeded 1%, the interface energy accompanied by the huge surface area of the nanomaterials made it difficult to homogeneously distribute and separate in liquid organic coatings. This led

to an obvious aggregation during curing and phase separation in the resulting film, thus decreasing the RCA abrasion performance of the coating films.

The organic solvent resistance rub testing reflected the chemical-resistance performance of the UV-cured coating, with ethanol and butanone being two typical solvents of concern in the 3C industry. Table 2 lists the testing results for every sample in different groups, with the number of scratches after the solvent resistance rub testing. No sample showed the phenomena of whitening and blistering, but the number of scratches increased with the loading of the bifunctional HEA-IPDI-HEA segments. Although the introduction of multi-functional modified CNTs and GO may increase the crosslinking density compared to the corresponding sample in the Ctrl group, the enhancement in the crosslinking density cannot match the density decrease caused by the increasing bifunctional HEA-IPDI-HEA segments. However, the CNT and GO themselves cannot improve the solvent-resistance property, so the results of the number of scratches increased following the loading of modified CNTs and GO in the cured coating film. Between ethanol and butanone, the coating in our system exhibited higher ethanol-resistance than did butanone. This is in agreement with the majority of polyurethane acrylate UV-curable coatings [3].

The boiling water resistance of the cured films is also shown in Table 2. It is observed that the cured films incorporated with carbon nanomaterials show an obvious improvement in boiling water resistance among the tested films. To our knowledge, the boiling water resistance mainly depends on the adhesion and the crosslinking density of the film. A good boiling water resistance can be obtained from films with good adhesion and high crosslinking density, which can be supplied by the trifunctional $(HDI\text{-}HECLA)_3$ and multi-functional modified carbon nanomaterials. Even an increase in the bifunctional HEA-IPDI-HEA segments decreased the crosslinking density in the Ctrl group. The introduction of a small amount of multi-functional carbon nanomaterials reversed the performance and dramatically improved the boiling water resistance of the samples in CNT and GO groups. Analogous to the RCA abrasion testing, a performance decrease was observed again in the samples that contained 1.0% CNT and GO, which was caused by the aggregation of nanomaterials and the phase separation phenomenon. In addition, it is believed that the hydrophobic property of CNTs and GO is contributory to the boiling resistance performance of our coating.

The gloss of samples containing carbon nanomaterials was lower because of the existence of the black CNTs and brown GO. The gloss suppression was increasingly heavy with increasing amounts of CNTs and GO in the film. For the Ctrl group without carbon nanomaterials, the samples kept nearly the same gloss value. The result agrees with the physical appearance shown in Figure 4a. Furthermore, when the concentration of carbon nanomaterials reached 1.0%, the gloss of the corresponding samples decreased dramatically, which was also caused by the aggregation of carbon nanomaterials.

Combining the property variations and the performance transformation, it was found that the introduction of modified CNTs and GO can improve the performance of UV-cured coatings to various degrees, depending on the exact concentration. The increased loading of these carbon nanomaterials causes a higher crosslinking density, resulting in an improved surface hardness, abrasion resistance, chemical-resistance performance and boiling water resistance. However, when too many CNTs and GO are introduced, the aggregations caused by the relatively large specific surface area of the nanomaterials have obvious effects, thus reducing these performances. Furthermore, the UV-curable coating exhibits a lower light transmissivity when more carbon nanomaterials are introduced, which influences the ultraviolet light absorbance and thus hinders the photopolymerization of the acrylates. This downgrade the performance of the UV-cured coatings. Therefore, it is very important to formulate a balanced content of carbon nanomaterials in a UV-curable coating to achieve the best performance.

4. Conclusions

With the combination of the trifunctional $(HDI\text{-}HECLA)_3$ with the bifunctional HEA-IPDI-HEA urethane acrylates as the reactive resin mixture and coordinated with TMPTA as the thinner, a novel UV-curable coating matrix was designed and prepared. The obtained coating system can be cured successfully under UV radiation to achieve excellent coatings on a PC substrate with good performances. By further introducing a relatively small amount of modified CNT and GO nanomaterials into the coating system, the performances, such as thermal stability, surface hardness, adhesion, abrasive resistance, and

chemical resistance, can be dramatically improved, and the composite coating can be potentially applied in the 3C industry as an excellent surface coating.

Acknowledgements

The authors acknowledge the support of Natural Science Foundation of China (No. 81671792), the support of National Key R&D program of China (2016YFC0104100). The works are also a part of the Project Funded by the Priority Academic Program Development of Jiangsu Higher Education Institutions (PAPD).

References

[1] Christmas B., Kemmerer R., Kosnik F.: UV/EB curing technology: A short history. in 'High performance polymers: Their origin and development' (eds.: Seymour R. B., Kirshenbaum G. S.) Springer, Dordrecht 331–337 (1986). https://doi.org/10.1007/978-94-011-7073-4_32

[2] Bongiovanni R., Sangermano M.: UV-curing science and technology. in 'Encyclopedia of polymer science and technology' (ed.: Mark H.) Wiley, New York, 1–20 (2002). https://doi.org/10.1002/0471440264.pst621

[3] Schwalm R.: Introduction to coatings technology. in 'UV coatings: Basics, recent developments and new applications' (ed.: Schwalm R.) Elsevier, Amsterdam, 1–18 (2007). https://doi.org/10.1016/B978-044452979-4/50001-9

[4] Ligon-Auer S. C., Schwentenwein M., Gorsche C., Stampfl J., Liska R.: Toughening of photo-curable polymer networks: A review. Polymer Chemistry, **7**, 257–286 (2016). https://doi.org/10.1039/C5PY01631B

[5] Xie J., Zhang N., Guers M., Varadan V. K.: Ultraviolet-curable polymers with chemically bonded carbon nanotubes for microelectromechanical system applications. Smart Materials and Structures, **11**, 575–580 (2002). https://doi.org/10.1088/0964-1726/11/4/313

[6] Ying F., Cui Y., Xue G., Qian H., Li A., Wang X., Zhang X., Jiang D.: Preparation and properties of an antistatic UV-curable coating modified by multi-walled carbon nanotubes. Polymer Bulletin, **73**, 2815–2830 (2016). https://doi.org/10.1007/s00289-016-1623-5

[7] Nayinia M. M. R., Bastani S., Moradian S., Croutxe-Barghorn C., Allonas X.: Rheological investigation of the gel time and shrinkage in hybrid organic/inorganic UV curable films. Journal of Photopolymer Science and Technology, **29**, 105–110 (2016). https://doi.org/10.2494/photopolymer.29.105

[8] Hu L., Yang Z., Zhang X., Liu Z., Xia P., Deng K., Gong L., Jiang L., Zhang H.: Fabrication and evaluation of dual function PMMA/nano-carbon composite particles for UV curable anti-glare coating. Progress in Organic Coatings, **101**, 81–89 (2016). https://doi.org/10.1016/j.porgcoat.2016.07.020

[9] Yazhini K. B., Prabu H. G.: Study on flame-retardant and UV-protection properties of cotton fabric functionalized with ppy–ZnO–CNT nanocomposite. RSC Advances, **5**, 49062–49069 (2015). https://doi.org/10.1039/C5RA07487H

[10] Kim S. R., Lee S. G., Yang J. M., Lee J. D.: Preparation and characterization of hybrid ozone resistance coating film using carbon nanotube. Polymer-Korea, **38**, 573–579 (2014). https://doi.org/10.7317/pk.2014.38.5.573

[11] Wright A. C., Faulkner M.: Magnetophoretic assembly and printing of nanowires. Journal of Vacuum Science and Technology B, Nanotechnology and Microelectronics: Materials, Processing, Measurement, and Phenomena, **30**, 021603/1–021603/7 (2012). https://doi.org/10.1116/1.3683152

[12] Ha H., Kim S. C., Ha K.: UV curing kinetics and properties of polyurethane acrylate/multi-walled carbon nanotube coatings. Macromolecular Research, **18**, 674–679 (2010). https://doi.org/10.1007/s13233-010-0705-8

[13] Sangermano M., Borella E., Priola A., Messori M., Taurino R., Pötschke P.: Use of single-walled carbon nanotubes as reinforcing fillers in UV-curable epoxy systems. Macromolecular Materials and Engineering, **293**, 708–713 (2008). https://doi.org/10.1002/mame.200800126

[14] Xu J., Cai X., Shen F.: Preparation and property of UV-curable polyurethane acrylate film filled with cationic surfactant treated graphene. Applied Surface Science, **379**, 433–439 (2016). https://doi.org/10.1016/j.apsusc.2016.04.104

[15] Barletta M., Vesco S., Puopolo M., Tagliaferri V.: Graphene reinforced UV-curable epoxy resins: Design, manufacture and material performance. Progress in Organic Coatings, **90**, 414–424 (2016). https://doi.org/10.1016/j.porgcoat.2015.08.013

[16] Yu B., Shi Y., Yuan B., Liu L., Yang H., Tai Q., Lo S., Song L., Hu Y.: Click-chemistry approach for graphene modification: Effective reinforcement of UV-curable functionalized graphene/polyurethane acrylate nanocomposites. RSC Advances, **5**, 13502–13506 (2015). https://doi.org/10.1039/C4RA15394D

[17] Barletta M., Vesco S., Puopolo M., Tagliaferri V.: High performance composite coatings on plastics: UV-curable cycloaliphatic epoxy resins reinforced by graphene or graphene derivatives. Surface and Coatings Technology, **272**, 322–336 (2015). https://doi.org/10.1016/j.surfcoat.2015.03.046

[18] Vitale A., Merlo S., Rizza G., Melilli G., Sangermano M.: UV Curing of perfluoropolyether oligomers containing graphene nanosheets to enhance water-vapor barrier properties. Macromolecular Chemistry and Physics, **215**, 1588–1592 (2014). https://doi.org/10.1002/macp.201400225

[19] Dai Y. T., Qiu F. X., Xu J. C., Yu Z. P., Yang P. F., Xu B. B., Jiang Y., Yang D. Y.: Preparation and properties of UV-curable waterborne graphene oxide/polyurethane-acrylate composites. Plastics, Rubber and Composites, **43**, 54–62 (2014). https://doi.org/10.1179/1743289813Y.0000000071

[20] Wang X., Xing W., Song L., Yu B., Hu Y., Yeoh G. H.: Preparation of UV-curable functionalized graphene/polyurethane acrylate nanocomposite with enhanced thermal and mechanical behaviors. Reactive and Functional Polymers, **73**, 854–858 (2013). https://doi.org/10.1016/j.reactfunctpolym.2013.03.003

[21] Pang B. L., Ryu C-M., Jin X., Kim H-I.: Preparation and properties of UV curable acrylic PSA by vinyl bonded graphene oxide. Applied Surface Science, **285**, 727–731 (2013). https://doi.org/10.1016/j.apsusc.2013.08.117

[22] Yu B., Wang X., Xing W., Yang H., Song L., Hu Y.: UV-curable functionalized graphene oxide/polyurethane acrylate nanocomposite coatings with enhanced thermal stability and mechanical properties. Industrial and Engineering Chemistry Research, **51**, 14629–14636 (2012). https://doi.org/10.1021/ie3013852

[23] Guo Y., Bao C., Song L., Qian X., Yuan B., Hu Y.: Radiation cured epoxy acrylate composites based on graphene, graphite oxide and functionalized graphite oxide with enhanced properties. Journal of Nanoscience and Nanotechnology, **12**, 1776–1791 (2012). https://doi.org/10.1166/jnn.2012.5185

[24] Brostow W., Lobland H. E., Hnatchuk N., Perez J. M.: Improvement of scratch and wear resistance of polymers by fillers including nanofillers. Nanomaterials, **7**, 66–78 (2017). https://doi.org/10.3390/nano7030066

[25] Hummers W. S., Offeman R. E.: Preparation of graphitic oxide. Journal of the American Chemical Society, **80**, 1339 (1958). https://doi.org/10.1021/ja01539a017

[26] Mishra R. S., Mishra A. K., Raju K. V. S. N.: Synthesis and property study of UV-curable hyperbranched polyurethane acrylate/ZnO hybrid coatings. European Polymer Journal, **45**, 960–966 (2009). https://doi.org/10.1016/j.eurpolymj.2008.11.023

[27] Seo J., Jang E-S., Song J-H., Choi S., Khan S. B., Han H.: Preparation and properties of poly(urethane acrylate) films for ultraviolet-curable coatings. Journal of Applied Polymer Science, **118**, 2454–2460 (2010). https://doi.org/10.1002/app.32344

[28] Jiao Z., Wang X., Yang Q., Wang C.: Modification and characterization of urethane acrylate oligomers used for UV-curable coatings. Polymer Bulletin, **74**, 2497–2511 (2016). https://doi.org/10.1007/s00289-016-1847-4